

Specific heat and exchange interactions of two isomer and isostructural copper–amino-acid complexes

Marcio L. Siqueira* and Raul E. Rapp

Instituto de Física, Universidade Federal do Rio de Janeiro, Caixa Postal 68528, Rio de Janeiro, 21945, Brazil

Rafael Calvo

*Instituto de Desarrollo Tecnológico para la Industria Química
and Facultad de Bioquímica y Ciencias Biológicas (CONICET-UNL),
Güemes 3450, 3000 Santa Fe, Argentina*

(Received 4 June 1992)

We report specific-heat measurements at temperatures in the range between 0.07 and 1.37 K of the isostructural copper–amino-acid isomer complexes Cu(L-but)_2 and Cu(D,L-but)_2 [$\text{Cu}(\text{H}_2\text{NCHCH}_2\text{CH}_2\text{CO}_2)_2$], which have copper ions in layers. No peaks that could indicate magnetic phase transitions are seen down to 0.07 K. The observed temperature dependences agree with the predictions of existing models for Heisenberg antiferromagnetic chains with nearest-neighbor isotropic exchange interactions. Values of the exchange-coupling parameter between copper ions of $J/k = (-0.64 \pm 0.01)$ and (-0.84 ± 0.01) K are obtained from the data in Cu(L-but)_2 and Cu(D,L-but)_2 , respectively. The one-dimensional behavior is interpreted as a consequence of predominant superexchange interactions connecting copper atoms along the \mathbf{b} axis through pairs of hydrogen bonds. Our results are compared with those obtained from the analysis of electron-paramagnetic-resonance-linewidth data for Cu(L-but)_2 and Cu(D,L-but)_2 , as well as with results from measurements in other copper–amino-acid complexes.

I. INTRODUCTION

Many recent experimental and theoretical studies of the magnetic properties of copper compounds have been focused on linear chains^{1–5} or layered⁶ spin systems, where the exchange interactions occur primarily in one or two dimensions. Analytical and numerical calculations of their thermodynamic and dynamic magnetic properties have been reported. They allow the evaluation of the exchange interactions from experimental data and analysis in terms of the lengths, angles, and nature of the bonds connecting the spins.

Copper–amino-acid complexes are convenient compounds to model properties of metal ions in copper proteins. Studies of their crystal structures, and electronic and magnetic properties are possible within the wide range of compounds with various crystal symmetries and bonding, which can be synthesized and crystallized. Understanding of the magnetostructural correlations observed in copper–amino-acid complexes may be useful in order to learn about superexchange at active sites of metalloproteins and enzymes, where exchange interactions between magnetically coupled metal ions essential for biological function have been observed.⁷

Many copper–amino-acid complexes may be classified as low-dimensional magnetic systems with copper ions in layers or chains, separated by the amino-acid molecules. The type which has attracted the most attention is Cu(aa)_2 , (where aa denotes amino acid), in which the copper ions are bonded to two amino-acid molecules in nearly square planar or elongated octahedral configurations. They consist of copper ions in layers,

having two magnetically nonequivalent copper sites (A and B) per unit cell, related by a 180° rotation around the monoclinic \mathbf{b} axis. Magnetic susceptibility, specific heat, and electron-paramagnetic-resonance (EPR) experiments in Cu(aa)_2 have shown an interesting low-dimensional magnetic behavior as a consequence of the spatial arrangement of the copper ions and the characteristics of the exchange paths connecting them.^{8–15} Since the values of the exchange parameter (J) are, in most cases, smaller than 1 K, their evaluation requires susceptibility or specific-heat measurements at very low temperatures.^{8,12,14} EPR linewidth data obtained in single-crystal samples at room temperature and more than one frequency are also useful to evaluate J .^{16,17} Values of the exchange interaction between neighbor copper ions at rotated crystal sites A and B , $|J_{AB}|$, obtained from EPR data in $\text{Cu(L-methionine)}_2$, Cu(L-leucine)_2 , and $\text{Cu(L-phenylalanine)}_2$ correlate well with the distances $d(\text{Cu-O}_{\text{ap}})$ between one copper and its nearest oxygen apical ligand, but show no correlations with the lengths and angles of hydrogen bonds bridging (AB) neighbor copper pairs.^{11,13} This observation has led us to conclude that carboxylate bridges provide the most important superexchange paths between (AB) pairs of copper ions in these complexes.^{11,13} This result was extrapolated and used to explain a predominantly one-dimensional (1D) magnetic behavior of Cu(L-alanine)_2 , indicated by susceptibility data at very low temperatures.¹⁴ EPR measurements cannot be used to evaluate the exchange interaction between magnetically equivalent neighbor copper ions, $|J_{AA}| = |J_{BB}|$, in Cu(aa)_2 ; only less accurate estimations were obtained by considering the broadening of the EPR

signal introduced by the hyperfine coupling with the copper nucleus.¹⁸

In order to obtain additional information about the exchange interactions in $\text{Cu}(\text{aa})_2$ we have performed specific-heat measurements in $\text{Cu}(\text{L-but})_2$ and $\text{Cu}(\text{D,L-but})_2$, the copper complexes of the amino acid *L*-2-aminobutyric acid and its *D,L* racemic mixture, in the very low-temperature range ($0.07 < T < 1.37$ K). These complexes are isomers having very similar crystal structures and were chosen for this investigation to observe in what extent these small structural differences influence the magnetic properties. Specific heat (C_{mag}) is a thermodynamic property with a relationship to the exchange interactions simpler than, for example, EPR data. It reflects the largest exchange interactions (and their sign), and not those between particular pairs of neighbor ions. Also, the specific heat is strongly related to the magnetic dimensionality of the system. Since the magnitudes of the exchange interactions in $\text{Cu}(\text{aa})_2$ are of the order of 1 K, they contribute to the specific heat in a range of temperature around or below this value, where the lattice contribution is negligible. This is very convenient in order to interpret the experimental results.

We found that the behavior of our C_{mag} vs T data for $\text{Cu}(\text{L-but})_2$ and $\text{Cu}(\text{D,L-but})_2$ is characteristic of 1D magnets, and fit well the predictions by Bonner and Fisher¹⁹ (BF), and of high- and low-temperature series expansions, for Heisenberg antiferromagnetic (AF) chains.^{20,21} This indicates that the magnitude of the coupling J_{AA} between equivalent copper neighbors is larger than the couplings J_{AB} . We evaluated J_{AA} and analyze them in terms of the characteristics of the hydrogen bonds connecting nearest-neighbor *AA* pairs, which, considering the crystallographic information,^{22,23} seem to be the dominant superexchange paths between copper ions. Our specific-heat results are discussed and compared with EPR measurements reported for $\text{Cu}(\text{L-but})_2$ and $\text{Cu}(\text{D,L-but})_2$.^{9,15,23,24}

II. EXPERIMENTAL DETAILS AND RESULTS

$\text{Cu}(\text{L-but})_2$ and $\text{Cu}(\text{D,L-but})_2$ were synthesized and crystallized as described previously.^{22,23} These materials, conveniently ground and sifted to $106\text{-}\mu\text{m}$ grain size, were mixed with copper powder ($5\mu\text{m}$) in a 1:1 volumetric ratio. Since the thermal conductivity of copper is much larger than those of $\text{Cu}(\text{L-but})_2$ and $\text{Cu}(\text{D,L-but})_2$, such a mixture ensures reasonable thermal equilibrium times. The sample holder (see Fig. 1) was made with two perforated copper sheets 0.01 mm thick, one rectangular (19×12 mm), and the other circular ($\phi = 9$ mm). The copper-sample mixture was sandwiched between the perforated copper foils, and pressed to about 25 MPa for about 30 min. Covering the copper foils with perforations increases the adherence of the surface in contact with the samples and speeds up the thermal response. This cylindrical sample holder, shown in Fig. 1, was sealed laterally and fixed with a small quantity of Stycast 1266 epoxy resin²⁵ to assure the integrity of the sample. The amounts of $\text{Cu}(\text{L-but})_2$ and $\text{Cu}(\text{D,L-but})_2$ in

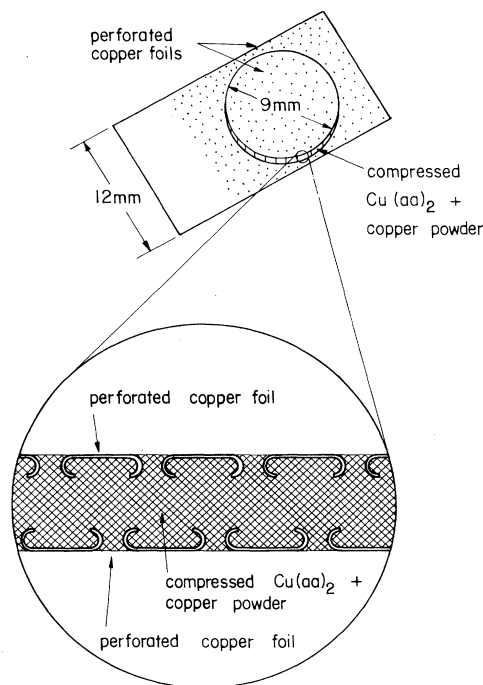


FIG. 1. Sample holder used for specific-heat measurements.

the samples were about 0.1 g.

The calorimeter used in this work was mounted below the mixing chamber of a ^3He - ^4He dilution refrigerator, and has been described previously by Rapp *et al.*²⁶ A carbon resistor, used as a thermometer,²⁷ was silver soldered to the rectangular copper foil,²⁶ while a commercial strain gage, fixed to the circular copper foil using GE 7031 varnish, was used as heater. The uncertainty on the thermometer calibration is less than 2%. The specific-heat measurements were performed using the standard adiabatic method, with linear extrapolations to the input and output drifts. The heating times of the samples were in the range 20–60 s, while the external time constant was of the order of hours. The temperature steps were made equal to 4% in the entire range. The system automation has been described elsewhere.²⁸

The values of C_{mag} were obtained after subtracting the heat capacity of the background, originated from copper foil and powder,^{26,29} Stycast 1266 resin,³⁰ and smaller components, to the measured heat capacity. At any temperature, the heat capacity of the background was equal to or smaller than 1% of the total heat capacity. These small contributions were evaluated with an uncertainty smaller than 10%, which introduces an error of less than 0.1% to the measured heat capacity of the sample. This value is similar to the uncertainty on the weights of $\text{Cu}(\text{L-but})_2$ and $\text{Cu}(\text{D,L-but})_2$ in the sample holder.

The experimental values of the specific heat C_{mag}/R for $\text{Cu}(\text{L-but})_2$ and $\text{Cu}(\text{D,L-but})_2$, obtained in the range $0.07 < T < 1.37$ K are displayed in Fig. 2. These C_{mag}/R vs T curves show broad maxima with $(C_{\text{mag}}/R)_{\text{max}} \approx 0.33$ at $T_{\text{max}} = 0.62$ and 0.81 K, respectively, and decay to zero as either $T \rightarrow 0$ or for $T > T_{\text{max}}$. This behavior is

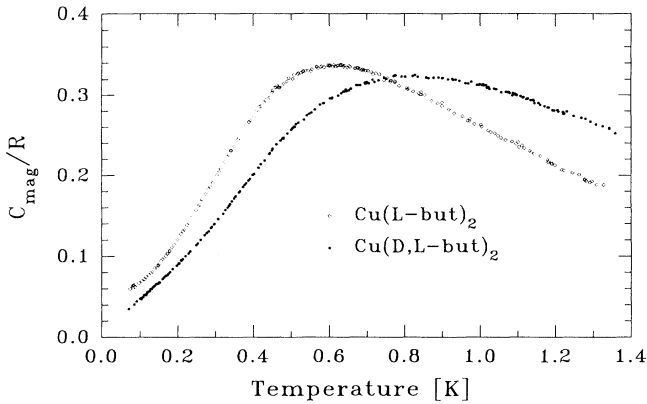


FIG. 2. Experimental values of the specific heat (C_{mag}/R) of Cu(L-but)₂ (open circles) and Cu(D,L-but)₂ (solid circles), shown together as a function of temperature T .

characteristic of low-dimensional magnetic systems where the short-range order is gradually reached with decreasing temperature. No peaks which may indicate phase transitions are observed. However, the $C_{\text{mag}}(T)/R$ curve for Cu(L-but)₂ changes the slope around $T=0.17$ K, which may anticipate a transition at lower T .

III. ANALYSIS OF THE DATA

The isotropic Heisenberg model is appropriate to explain the exchange interactions in most Cu(II) compounds, where the spin Hamiltonian is usually written as²

$$\mathcal{H} = -2 \sum_{i>j} J_{ij} \mathbf{S}_i \cdot \mathbf{S}_j. \quad (1)$$

In Eq. (1), \mathbf{S}_i is the spin at the i lattice site ($S=\frac{1}{2}$ for copper ions), and each spin pair i,j with exchange interaction J_{ij} is counted only once; $J_{ij} < 0$ holds for anti-ferromagnetic and $J_{ij} > 0$ for ferromagnetic (FM) interactions. The thermodynamic properties can be calculated using the Hamiltonian of Eq. (1), with appropriate values of the J_{ij} . However, there is no formal solution to this problem for a real infinite lattice. Bonner and Fisher¹⁹ reported numerical calculations of the susceptibility and specific heat of AF and FM finite chains of up to 11 spins $S=\frac{1}{2}$, considering the exchange interactions between nearest-neighbor spins ($J_{ij}=J$ for $i=j\pm 1$ and $J_{ij}=0$ otherwise). The extrapolation of these results to infinite chains explains well experimental data for many chain compounds.² In the case of AF isotropic Heisenberg infinite chains they predict a broad peak with a maximum value $(C_{\text{mag}}/R)_{\text{max}}=0.3497$ at $kT_{\text{max}}/|J|=0.961$. No phase transitions exist for $T > 0$. At $T \ll T_{\text{max}}$, the BF result for an AF chain,

$$C_{\text{mag}}/R = 0.35 \frac{kT}{|J|},$$

agrees well with the result of Takahashi,²¹ $C_{\text{mag}}/R = kT/3|J|$, obtained with spin-wave theory (SWT). At $T > T_{\text{max}}$, the BF results agree well with the

prediction obtained using Padé approximants of high-temperature series expansions (HTSE) for 1D chains.²⁰ Numerical values for $C_{\text{mag}}(T)/R$ obtained by the method of BF, together with those predicted by SWT and HTSE, have been tabulated by Blöthe.³¹ They resemble well our results for Cu(L-but)₂ and Cu(D,L-but)₂, and were used to fit the data in Fig. 2. Good agreement is obtained with values of the nearest-neighbor exchange parameters J :

$$J_{\text{BF}}^L/k = (-0.64 \pm 0.01)\text{K} \text{ for Cu(L-but)}_2$$

and

$$J_{\text{BF}}^{\text{DL}}/k = (-0.84 \pm 0.01)\text{K} \text{ for Cu(D,L-but)}_2,$$

as the single adjustable parameter. The uncertainties on these values were estimated from the dispersion of the fits. In Fig. 3, we compare the experimental values of C_{mag}/R as a function of T for Cu(L-but)₂ [Fig. 3(a)] and Cu(D,L-but)₂ [Fig. 3(b)] with those predicted for the AF chain with nearest-neighbor exchange interactions.³¹ The temperature variation of C_{mag} predicted by the BF model for FM chains has a totally different shape and cannot be used to fit our data.

Since in Cu(L-but)₂ and Cu(D,L-but)₂ the copper ions are arranged in layers, we have also attempted to fit our specific-heat data with existing predictions for spin layers. There is no numerical solution comparable to the BF solution for a 1D lattice to the problem of a 2D spin sys-

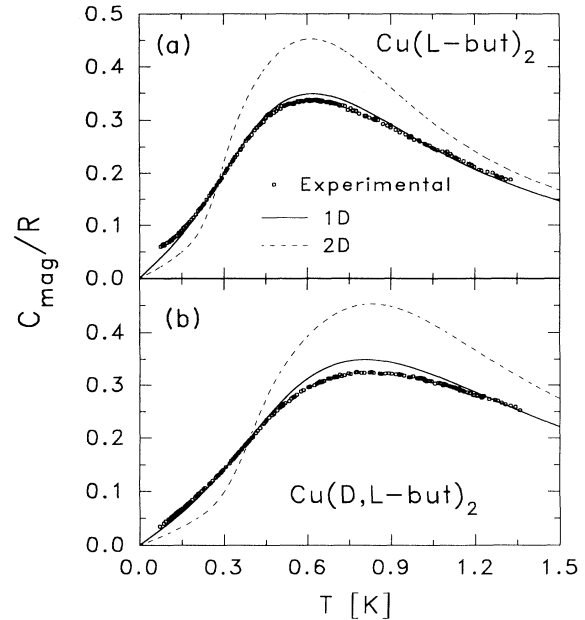


FIG. 3. Experimental values of the specific heat (C_{mag}/R) of Cu(L-but)₂ (a) and Cu(D,L-but)₂ (b) shown as a function of temperature. The solid lines indicate the model predictions for AF chains. Values $J/k = -0.64$ K and $J/k = -0.84$ K are obtained from least-squares fits for the single adjustable parameter for Cu(L-but)₂ and Cu(D,L-but)₂. The dashed lines are the predictions for the 2D square planar AF which reproduce the experimental values of T_{max} .

tem coupled by isotropic exchange. High-temperatures series expansions using Padé approximation techniques³²⁻³⁵ have been used to calculate the susceptibility and the specific heat in 2D magnetic systems at temperatures $T/T_{\max} > 1$. Baker *et al.*,³² and Navarro *et al.*,³³ obtained a maximum $(C_{\text{mag}}/R)_{\text{max}} \cong 0.45$ in the specific-heat curve of the AF square planar layer at $kT_{\text{max}}/|J| \cong 1.3$, while Yamaji and Kondo,³⁴ and Bloembergen,³⁵ obtained for the square planar FM layer a maximum $(C_{\text{mag}}/R)_{\text{max}} \cong 0.38$ at $kT_{\text{max}}/|J| \cong 0.8$. Algra, de Jongh, and Carlin³⁶ illustrated the differences between specific-heat curves for 1D and 2D AF arrays considering experimental results for $\text{CuL}_6(\text{ClO}_4)_2$ and $\text{CuL}_6(\text{BF}_4)_2$ ($L = \text{C}_5\text{H}_5\text{NO}$). SWT has been used in the low- T range ($T/T_{\text{max}} < 0.1$) to predict $C_{\text{mag}}/R \propto (kT/J)^2$ for quadratic spin layers.³⁷⁻³⁹ These predictions for 2D magnetic lattices, particularly the value of $(C_{\text{mag}}/R)_{\text{max}}$ and the temperature dependence for $T \ll T_{\text{max}}$, differ from the behavior of our specific-heat data for $\text{Cu}(\text{L-but})_2$ and $\text{Cu}(\text{D,L-but})_2$. This is in contrast with the good agreement obtained with the 1D AF chain, displayed by Figs. 3(a) and 3(b). In order to stress the inadequacy of the 2D AF model to fit our experimental results in $\text{Cu}(\text{L-but})_2$ and $\text{Cu}(\text{D,L-but})_2$, we display with dashed lines in Figs. 3(a) and 3(b) the predictions for the 2D square planar AF reported by Navarro³³ for values of the exchange interaction parameter J which reproduce the observed T_{max} .

IV. STRUCTURES OF $\text{Cu}(\text{L-but})_2$ AND $\text{Cu}(\text{D,L-but})_2$

Full crystallographic studies of $\text{Cu}(\text{D,L-but})_2$ and $\text{Cu}(\text{L-but})_2$ were reported by Fawcett *et al.*²² and Levstein *et al.*²³ The main features of these molecular and crystal structures are illustrated in Fig. 4. The relevant

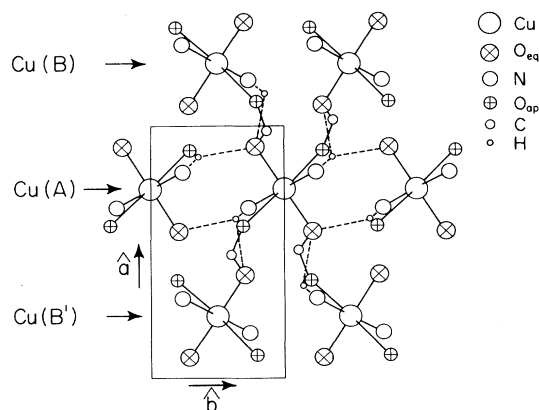
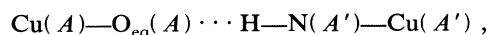


FIG. 4. Structure of the copper layers in $\text{Cu}(\text{L-but})_2$ and $\text{Cu}(\text{D,L-but})_2$, as obtained from the crystallographic data. Hydrogen bonds from the central $\text{Cu}(A)$ are indicated with dashed lines. $\text{Cu}(A)$ and $\text{Cu}(B)$ indicate the two (rotated) copper sites in the structure. B and B' are identical sites and differ only in their position relative to a particular site A . The size of the unit cell of the crystal is indicated. The oxygens bound apically and equatorially to the copper ions are labelled O_{ap} and O_{eq} , respectively.

structural parameters are given in Table I. The two rotated (but otherwise equivalent) copper ions A and B per unit cell are in a square planar transcoordination with a N_2O_2 ligand set. Two oxygens from carboxylate groups of other amino-acid molecules act as apical ligands and complete an elongated octahedral coordination around the copper. These octahedra are arranged in layers (shown in Fig. 4). The distance between neighbor copper atoms in a layer is of the order of 5 Å, while the distance between layers is approximately 11 Å. Table I shows the small differences in the copper-ligand distances between $\text{Cu}(\text{L-but})_2$ and $\text{Cu}(\text{D,L-but})_2$.

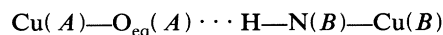
The chemical paths which may provide superexchange links between copper ions in $\text{Cu}(\text{L-but})_2$ and $\text{Cu}(\text{D,L-but})_2$ [and in most $\text{Cu}(\text{aa})_2$] are the following.

(i) Pairs of H bonds connecting nearest-neighbors (AA) or (BB) copper pairs through their equatorial ligands,

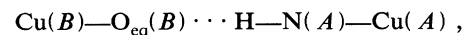


as described in Figs. 4 (dashed lines) and 5. These two hydrogen bonds are identical (symmetry related) in $\text{Cu}(\text{D,L-but})_2$ but slightly different in $\text{Cu}(\text{L-but})_2$ (Fig. 5). The relevant distances and angles for $\text{Cu}(\text{L-but})_2$ and $\text{Cu}(\text{D,L-but})_2$ are included in Fig. 5, as obtained from the crystallographic studies.^{22,23}

(ii) Hydrogen bonds, connecting equatorial oxygen and nitrogen ligands of an A -type copper, to equatorial nitrogen and oxygen ligands of the four neighbor B -type coppers,



and



which are indicated in Fig. 4 as dashed lines.

TABLE I. Values of structural parameters of $\text{Cu}(\text{L-but})_2$ and $\text{Cu}(\text{D,L-but})_2$, as obtained from the x-ray studies (Refs. 22 and 23). The labeling of the crystal axes of $\text{Cu}(\text{D,L-but})_2$ used in Ref. 22 has been changed to simplify the comparison.

System	$\text{Cu}(\text{L-but})_2$	$\text{Cu}(\text{D,L-but})_2$
Space group	$P2_1$	$P2_1/c$
a [Å]	9.464	9.487
b [Å]	5.060	5.066
c [Å]	11.189	11.13
β (deg)	90.60	92.15
Z	2	2
Interlayer dist.	11.18	11.13
Distances $\text{Cu}(A) - \text{Cu}(A)$	5.060	5.066
Distances $\text{Cu}(A) - \text{Cu}(B)$	5.34	5.38
	5.41	
$\text{Cu} - \text{O}_{\text{eq}}$	1.955	1.947
	1.962	
$\text{Cu} - \text{O}_{\text{ap}}$	2.787	2.758
	2.679	

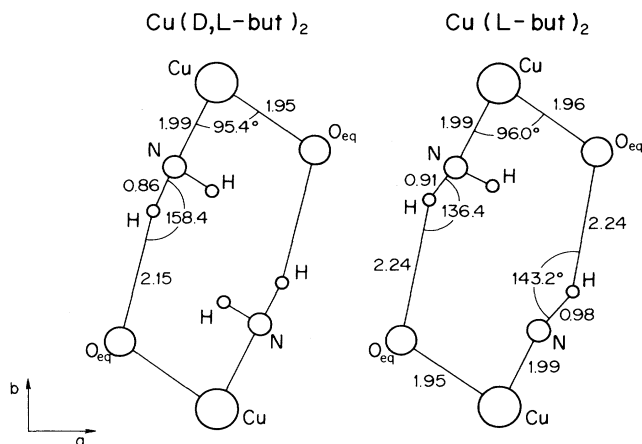
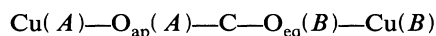
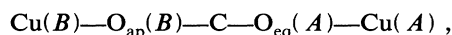


FIG. 5. Structure, distances, and angles of the two H bonds connecting two AA (or BB) neighbor copper ions in Cu(L-but)_2 and Cu(D,L-but)_2 . In the case of Cu(D,L-but)_2 the crystal symmetry imposes equal distances and angles to these bonds.

(iii) Carboxylate bridges



and



which are shown in Fig. 4, connect an apical oxygen ligand O_{ap} to one copper, with an equatorial oxygen O_{eq} ligand to the nearest-neighbor copper of a different type. The inversion point symmetry at the copper atoms, which exists in Cu(D,L-but)_2 (space group $P2_1/c$), does not exist in Cu(L-but)_2 (space group $P2_1$). Then, the distances (and paths) between one copper and its two apical ligands are different, and the superexchange paths between one type A - (B -) copper and its four type B - (A -) copper neighbors of different type are different by pairs in Cu(L-but)_2 .

V. DISCUSSION

A 1D magnetic behavior of layered compounds may arise from the nonequivalence of the exchange paths along different directions within the spin layers. We now interpret the good fit of the specific-heat data with the predictions for an isotropic AF chain showed in Figs. 3(a) and 3(b), in terms of the structures of Cu(L-but)_2 and Cu(D,L-but)_2 . The values of the exchange coupling parameters obtained from the specific-heat data in Cu(L-but)_2 and Cu(D,L-but)_2 are then compared with EPR results in the same compounds.^{15,23}

A. Magnetic dimension of the systems

According to the crystallographic data,^{22,23} the exchange paths between AA or BB pairs of copper neighbors along the b axis are pairs of hydrogen bonds (see Figs. 4 and 5), which determine the value of $J_{AA} = J_{BB}$. On the other hand, hydrogen bonds and carboxylate

bridges, connecting an A - (B -) type copper with its four B - (A -) type copper neighbors (Fig. 4), acting together as superexchange paths, determine the value of J_{AB} . It was concluded in a previous EPR study of three other Cu(aa)_2 ,¹³ that at room temperature the most important contribution to J_{AB} arises from the carboxylate bridges. However, it was not clear if this conclusion holds for Cu(L-but)_2 and Cu(D,L-but)_2 .^{15,23} The distances between copper layers in these two compounds are much shorter than those for the complexes analyzed in Ref. 13. Since the evaluation of exchange parameters from EPR data strongly depends on magnetic dimension, the values of the exchange parameters obtained in Cu(L-but)_2 and Cu(D,L-but)_2 cannot be safely compared with those for the other complexes.

Considering that copper layers in ab planes separated by 11.1 Å are well isolated, the magnetic dimensionality of Cu(L-but)_2 and Cu(D,L-but)_2 is mainly a consequence of the relative magnitudes of J_{AA} and J_{AB} . The AA (BB) superexchange couplings J_{AA} alone would produce a 1D magnetic behavior of both Cu(L-but)_2 and Cu(D,L-but)_2 , with chains along the b axis. For $J_{AB} = 0$ there would be no spin correlation between coppers in adjacent chains. On the other hand, the AB exchange couplings J_{AB} may produce different behaviors in Cu(D,L-but)_2 and Cu(L-but)_2 . In Cu(D,L-but)_2 , a type- A copper ion is equally connected with its four rotated B -type copper neighbors within the layer, and a 2D behavior would be expected if $|J_{AB}| \gg |J_{AA}|$. However, the behavior will still be 1D if $|J_{AA}| \gg |J_{AB}|$. In the case of Cu(L-but)_2 the couplings J_{AB} between a $\text{Cu}(A)$ and the two nearest neighbors $\text{Cu}(B)$ and between $\text{Cu}(A)$ and the two nearest neighbors $\text{Cu}(B')$ on the other side (see Fig. 4) may be different. In this case the magnetic dimensionality would be in between 2D and 1D, depending on J_{AA} and also on the differences between the superexchange paths connecting a $\text{Cu}(A)$ and its two nearest neighbors $\text{Cu}(B)$ and those connecting $\text{Cu}(A)$ and the other two nearest-neighbors $\text{Cu}(B')$. As discussed in previous papers,^{14,15} these differences in J_{AB} may produce a 2D array of weakly coupled 1D zigzag chains.

B. The magnitudes of the exchange

The 1D magnetic behavior shown by the specific-heat data for both L and D,L compounds can be understood if $|J_{AA}| \gg |J_{AB}|$ for Cu(L-but)_2 and Cu(D,L-but)_2 . Then, the values

$$J_{BF}^L/k = (-0.64 \pm 0.01) \text{ K}$$

and

$$J_{BF}^{DL}/k = (-0.84 \pm 0.01) \text{ K}$$

are interpreted as the magnitudes of the exchange couplings arising from the pairs of H bonds bridging AA neighbor copper pairs along the b axis. These hydrogen bridges are shorter, and with an angle closer to 180° in the case of Cu(D,L-but)_2 (see Fig. 5). Consequently, they are stronger and able to produce the larger exchange coupling between AA neighbor copper pairs observed in this

compound. Also, since the two AA H bridges are identical in $\text{Cu}(\text{D,L-but})_2$, their effects add up, while the differences between them in $\text{Cu}(\text{L-but})_2$ produce an interference, which might reduce the magnitude of J_{AA} .^{40,41}

The small discrepancies between the maximum observed values of C_{mag}/R [0.338 at 0.62 K for $\text{Cu}(\text{L-but})_2$, and 0.325 at 0.81 K for $\text{Cu}(\text{D,L-but})_2$], in comparison to the prediction by BF for the AF chain (0.3497),^{5,19} may be due to small out-of-chain superexchange interactions.

C. Comparison with the EPR results

A large amount of information about the magnetic interactions in $\text{Cu}(\text{aa})_2$ has been obtained previously by EPR. Therefore, we consider it useful to include here a discussion about these findings, and a comparison with the present results. To analyze EPR data in paramagnets one uses the linear response and “exchange narrowing” theories introduced by Anderson⁴² and Kubo and Tomita⁴³ (see also Ref. 44). The observed linewidth is related to integrals of time correlation functions between spin operators, and then to the spin dynamics, determined by the magnitude of $|J|$. For relatively narrow resonances, the EPR linewidth mainly depends on the long-time behavior in the spin dynamics, where the spin correlation functions are governed by diffusion processes.⁴⁵ Since diffusion is strongly dependent on dimension, EPR linewidth measurements allow one to detect changes in the magnetic dimensionality produced by small changes in the crystal structures of $\text{Cu}(\text{aa})_2$.¹⁵ The negative aspect of EPR as a technique to evaluate exchange interactions is the complicated relationship of the values of $|J|$ with the angular variation of the linewidth. Positive aspects are that $|J|$ values of the order of tenths of K may be evaluated at room temperature, and that EPR provides, in some cases, a selective method to evaluate exchange couplings between specific spins within the unit cell, instead of a bulk, averaged value.

The EPR studies at 35 GHz (Refs. 15 and 23) in $\text{Cu}(\text{L-but})_2$ and in $\text{Cu}(\text{D,L-but})_2$ allow one to evaluate $|J_{AB}|$. A difference between the Zeeman terms in the Hamiltonian of the A - and B -type copper ions is produced by the different orientation of their g tensors. In the absence of exchange J_{AB} , two lines should be observed at g_A and g_B . The AB exchange interaction collapses these two resonances at $g = (g_A + g_B)/2$. However, the difference between g_A and g_B is still present as a contribution to the linewidth proportional to the square of the difference in Zeeman energies (then, to the square of the microwave frequency) and to the inverse of the exchange coupling $|J_{AB}|$.^{16,17} This allows one to evaluate $|J_{AB}|$ by extracting this contribution from the angular variation of the linewidth, performing experiments at different frequencies. According to our definition of J in Eq. (1),⁴⁶ the values obtained for $|J_{AB}|$ from the EPR data are

$$|J_{AB}^L|/k = 0.18 \text{ K}$$

and

$$|J_{AB}^{DL}|/k = 0.29 \text{ K},$$

which are about three times smaller than the values of J_{AA} obtained for the same systems from the present specific-heat data. These relatively small factors do not justify the 1D behavior observed in Fig. 3. In fact, these values of J_{AB} should produce much larger deviations towards to the 2D behavior discussed before. Since the EPR results were obtained at room T , a possible explanation may be a strong temperature dependence of the exchange parameters. Changes with T of the exchange coupling have been reported by several authors.^{47,48} The behavior observed in most cases is an increase of $|J|$ with decreasing T , due to an increase of the unpaired electron overlap when the lattice contracts. However, reduction of $|J|$ with decreasing T has also been reported.⁴⁸ It was attributed to the result of a competition between FM and AF contributions to the exchange, having similar magnitudes. The antiferromagnetic contribution is very sensitive to distances and geometry, which change with temperature. Then, the net result for $d|J|/dT$ may be positive or negative, depending on the relative magnitudes of AF and FM contributions.⁴⁸

It is interesting to discuss the transition from a 1D to a 2D spin dynamics, going from $\text{Cu}(\text{L-but})_2$ to $\text{Cu}(\text{D,L-but})_2$, which was concluded from the EPR linewidth data.¹⁵ This dimensionality refers specifically to the AB exchange coupling detected by EPR and is not related to the bulk 1D magnetic behavior observed in both systems in our specific-heat data. In this sense EPR allows a sensitive separation of the effects of exchange couplings between magnetically nonequivalent ions in the lattice.

D. Superexchange interactions through H bonds

A result of our present study is the evaluation of the exchange coupling between two coppers connected equatorially by a pair of hydrogen bonds (see Fig. 5). Very little is known about the effectiveness of hydrogen bonds for superexchange. We are not aware of theoretical studies on superexchange interactions through H bonds which may be compared to our results. Carlin² analyzes magnetostructural correlations observed in several materials where the important paths for superexchange are H bonds. However, in our opinion, the known results are not yet enough to draw conclusions about copper–amino-acid complexes. Since H bonds are very important in biomolecules, it would be interesting to find out whether the order of magnitude in the observed couplings (0.5–1 K) can be taken as an estimate for other systems. Hoffmann *et al.*¹⁰ determined a value $|J|/k = 0.006 \text{ K}$ for the coupling between copper ions apically connected by H bonds in copper(cis-glycine)₂. Since the electronic density between copper and its apical ligands is very small, a drastic reduction of J is expected in this case, and then this result is compatible, but not comparable, with ours.

Recent specific-heat measurements in $\text{Cu}(\text{L-ile})_2$, another copper–amino-acid complex having coppers in layers and no carboxylate bridges for AB superexchange, also seem to indicate a 1D behavior.¹² However, the existence of a phase transition peak at a temperature close to that of the maximum expected for a 1D chain makes a

more detailed analysis of the magnetic dimensionality of this compound difficult.

E. The possibility of frustration effects

Looking at Fig. 4 it is easy to imagine that if the exchange interaction J_{AA} between AA neighbor copper pairs is AF, there would be frustration effects for any sign and non-negligible magnitude of J_{AB} . However, these effects do not seem to show up in our specific-heat results.

It would be interesting to have very low- T susceptibility data to be able to analyze this possibility.

ACKNOWLEDGMENTS

We are grateful to Dr. Patricia Levstein for her collaboration in the synthesis of the compounds, and to Dr. J. Saunders and Dr. M. Passeggi for their comments on the manuscript. This work has been supported by CNPq and FINEP (Brazil) and by CONICET and Fundación Antorchas (Argentina).

*Present address: Millikelvin Laboratory, Royal Holloway and Bedford New College, University of London, Egham Hill, Egham, Surrey, TW20 OEX, United Kingdom.

¹L. J. de Jongh and A. R. Miedema, *Adv. Phys.* **23**, 1 (1974).

²R. Carlin, *Magnetochemistry* (Springer, Berlin, 1986).

³*Magneto Structural Correlations in Exchange Coupled Systems*, edited by R. D. Willet, D. Gatteschi, and O. Kahn, NATO Advanced Study Institute Series C Vol. 140 (Reidel, Dordrecht, 1984).

⁴L. J. de Jongh, in *Magneto Structural Correlations in Exchange Coupled Systems* (Ref. 3), pp. 1–35.

⁵J. C. Bonner, in *Magneto Structural Correlations in Exchange Coupled Systems* (Ref. 3), pp. 157–205.

⁶*Magnetic Properties of Layered Transition Metal Compounds*, edited by L. J. de Jongh (Kluwer Academic, Dordrecht 1989).

⁷E. I. Solomon and D. E. Wilcox, in *Magneto Structural Correlations in Exchange Coupled Systems* (Ref. 3), pp. 463–496.

⁸P. R. Newman, J. L. Imes, and J. A. Cowen, *Phys. Rev. B* **13**, 4093 (1976).

⁹R. Calvo and M. A. Mesa, *Phys. Rev. B* **28**, 1244 (1983).

¹⁰S. K. Hoffmann, J. Gozlar, and L. S. Sczepaniak, *Phys. Rev. B* **37**, 7331 (1988).

¹¹P. R. Levstein, Ph.D. thesis, Universidad Nacional del Litoral, Argentina, 1989 (unpublished).

¹²T. Wakamatsu, T. Hashiguchi, M. Nakano, M. Sorai, H. Suga, and Tan Zhi-Cheng, *Chin. Sci. Bull.* **34**, 1795 (1989).

¹³P. R. Levstein and R. Calvo, *Inorg. Chem.* **29**, 1581 (1990).

¹⁴R. Calvo, M. C. G. Passeggi, M. A. Novak, O. G. Symko, S. B. Oseroff, O. R. Nascimento, and M. C. Terrile, *Phys. Rev. B* **43**, 1074 (1991).

¹⁵P. R. Levstein, H. M. Pastawski, and R. Calvo, *J. Phys.: Condens. Matter* **3**, 1877 (1991).

¹⁶M. Yokota and S. Koide, *J. Phys. Soc. Jpn.* **9**, 953 (1954).

¹⁷P. R. Levstein, C. A. Steren, A. M. Gennaro, and R. Calvo, *Chem. Phys.* **120**, 449 (1988).

¹⁸R. Calvo, H. Isern, and M. A. Mesa, *Chem. Phys.* **100**, 89 (1985).

¹⁹J. C. Bonner and M. E. Fisher, *Phys. Rev.* **135**, A640 (1964).

²⁰G. A. Baker, Jr., G. S. Rushbrooke, and H. E. Gilbert, *Phys. Rev.* **135**, A1272 (1964).

²¹M. Takahashi, *Prog. Theor. Phys.* **50**, 1519 (1973).

²²T. G. Fawcett, M. Ushay, J. P. Rose, R. A. Lalancette, J. A. Potenza, and H. J. Shugar, *Inorg. Chem.* **18**, 327 (1979); an early two-dimensional x-ray structural study of $\text{Cu}(\text{D,L-but})_2$ was reported by A. J. Stosick, *J. Am. Chem. Soc.* **67**, 362 (1945).

²³P. R. Levstein, R. Calvo, E. E. Castellano, O. E. Piro, and B.

E. Rivero, *Inorg. Chem.* **29**, 3918 (1990).

²⁴R. Calvo and M. A. Mesa, *Phys. Lett.* **108A**, 217 (1985).

²⁵Emerson & Cuming Inc., Canton, MA 02021.

²⁶R. E. Rapp, M. L. Siqueira, R. J. Viana, and L. C. Norte, *Rev. Sci. Instrum.* **63**, 5390 (1992).

²⁷M. L. Siqueira, R. J. Viana, and R. E. Rapp, *Cryogenics* **31**, 796 (1991).

²⁸M. L. Siqueira, R. E. Rapp, and F. A. B. Chaves, *Rev. Fis. Apl. Instrum.* **5**, 401 (1990).

²⁹N. E. Phillips, *Phys. Rev.* **134**, A385 (1964); R. J. Schutz, *Rev. Sci. Instrum.* **45**, 548 (1974).

³⁰M. L. Siqueira and R. E. Rapp, *Rev. Sci. Instrum.* **62**, 2499 (1991).

³¹H. W. J. Blöthe, *Physica* **78**, 302 (1974); *Physica B* **79**, 427 (1975).

³²G. A. Baker, Jr., H. E. Gilbert, J. Eve, and G. S. Rushbrooke, *Phys. Lett.* **27A**, 2 (1968).

³³R. Navarro, H. A. Algra, L. J. de Jongh, R. L. Carlin, and C. J. O'Connor, *Physica B* **86-88**, 693 (1977).

³⁴K. Yamaji and J. Kondo, *J. Phys. Soc. Jpn.* **35**, 25 (1973).

³⁵P. Bloembergen, *Physica B* **85**, 51 (1977).

³⁶H. A. Algra, L. J. de Jongh, and R. L. Carlin, *Physica B* **93**, 24 (1978); *Physica B+C* **95**, 224 (1978).

³⁷P. W. Anderson, *Phys. Rev.* **86**, 694 (1952).

³⁸R. Kubo, *Phys. Rev.* **87**, 568 (1952).

³⁹A. F. M. Arts and H. W. DeWijn, in *Magnetic Properties of Layered Transition Metal Compounds* (Ref. 6), pp. 191–229.

⁴⁰P. J. Hay, J. C. Thibeault, and R. J. Hoffmann, *J. Am. Chem. Soc.* **97**, 4884 (1975).

⁴¹P. R. Levstein, H. M. Pastawski, and J. L. D'Amato, *J. Phys.: Condens. Matter* **2**, 1781 (1990).

⁴²P. W. Anderson, *J. Phys. Soc. Jpn.* **9**, 316 (1954).

⁴³R. Kubo and K. Tomita, *J. Phys. Soc. Jpn.* **9**, 888 (1954).

⁴⁴A. Bencini and D. Gatteschi, *Electron Paramagnetic Resonance of Exchange Coupled Systems* (Springer, Berlin, 1989).

⁴⁵P. M. Richards, in *Local Properties at Phase Transitions*, Proceedings of the International School of Physics "Enrico Fermi," Course XIL, Varenna, 1973, edited by K. D. Mueller and A. Rigamonti (North-Holland, Amsterdam, 1976).

⁴⁶The values of $|J_{AB}|$ for $\text{Cu}(\text{L-but})_2$ and $\text{Cu}(\text{D,L-but})_2$ reported in Refs. 15 and 23 have to be divided by two to conform to our definition of Eq. (1).

⁴⁷S. K. Hoffmann, *Chem. Phys. Lett.* **98**, 329 (1983).

⁴⁸S. K. Hoffmann, A. Waskowska, and W. Hilczer, *Solid State Commun.* **74**, 1359 (1990); S. K. Hoffmann and W. Hilczer, *Inorg. Chem.* **30**, 2210 (1991), and references therein.